Nuclear Engineering and Technology 52 (2020) 610–613

Contents lists available at ScienceDirect

Nuclear Engineering and Technology

journal homepage: www.elsevier.com/locate/net

Original Article

Irradiation-induced BCC-phase formation and magnetism in a 316 austenitic stainless steel

Chaoliang Xu, Xiangbing Liu*, Fei Xue**, Yuanfei Li, Wangjie Qian, Wenqing Jia

Suzhou Nuclear Power Research Institute, Suzhou, Jiangsu province, 215004, China

ARTICLE INFO

Article history:
Received 19 March 2019
Received in revised form
14 August 2019
Accepted 4 September 2019
Available online 5 September 2019

Keywords:
Irradiation
Austenitic stainless steel
BCC-Phase formation

ABSTRACT

Specimens of austenitic stainless steel were irradiated with 6 MeV Xe ions to two doses of 7 and 15 dpa at room temperature and 300 °C respectively. Then partial irradiated specimens were subsequently thermally annealed at 550 °C. Irradiation-induced BCC-phase formation and magnetism were analyzed by grazing incidence X-ray diffraction (GIXRD) and vibrating sample magnetometer (VSM). It has been shown that irradiation damage level, irradiation temperature and annealing temperature have significant effect on BCC-phase formation. This BCC-phase changes the magnetic behavior of austenitic stainless steel. The stress relief and compositional changes in matrix are the driving forces for BCC-phase formation in austenitic stainless steel during ion irradiation.

1. Introduction

Austenitic stainless steels (ASS) are essential structural materials and widely used in core internals of fission reactor. Irradiation-assisted stress corrosion cracking (IASCC) is one of the most important degradation mechanisms in core internals. It is known that the BCC-phase formation in ASS may be induced by ion irradiation. Previous studies have suggested that the BCC-phase and IASCC can be detected simultaneously in irradiated ASS [1] BCC-phase formation in ASS may be one of the important influencing factors of IASCC susceptibility [2]. Therefore, the investigation of the BCC-phase formation mechanism in ASS can provide crucial information for the understanding of IASCC phenomenon.

Previously, different kinds of ions were used in several studies to investigate BCC-phase formation in ASS. But these studies mainly focus on the analysis of phase formation phenomenon and its morphology under different irradiation damage level [3,4]. Few analyses have been conducted to determine the BCC-phase volume fraction and its evolution at different irradiation condition and annealing temperature. So the driving force of BCC-phase formation under irradiation is still not clear. On the other hand, many investigations have examined the reverse of BCC-phase to austenite phase in cold worked and irradiated ASS, while the effect of irradiation temperature and post irradiation annealing (PIA) on BCC-phase formation is very limited.

In the present study, the synchrotron radiation grazing incidence X-ray diffraction (GIXRD) was used to confirm the formation of BCC-phase. Then the volume fraction of BCC-phase induced by irradiation was analyzed by the vibrating sample magnetometer (VSM). Finally, the driving force of the irradiation-induced BCC-phase was discussed in detail.

2. Experiments

The material used in this study is 316 ASS with solution treatment at 1060 °C for 90 min. The chemical composition is Cr (17.28%), Ni (11.65%), Mo (2.49%), Mn (1.24%), Cu (0.46%), Si (0.340%), C (0.038%), Co (0.010%), P (0.008%), S (0.003%) and Fe (the balance).

Firstly, the specimens were mechanically polished by the silicon carbide paper with various grades of 800–2000 and 0.5 μm diamond spray until a mirror-like surface appeared before irradiation. Then these specimens were irradiated with Xe ions to 2.3×10^{15} and 5×10^{15} Xe/cm^2 at room temperature (RT) and 300 °C respectively at the ECR-320 kV High-voltage Platform in the Institute of Modern Physics, Chinese Academy of Science. During the irradiation process, the Xe ions flux is about 2.6×10^{11} ion/cm^2•s and the vacuum degree in specimen chamber is better than 1×10^{-5} Pa. According to the theoretical calculation by Monte-Carlo code SRIM 2012 [5] (taking the density of 7.8 g/cm^3 and threshold displacement energies of 40 eV for Fe, Cr and Ni sub-

* Corresponding author.
** Corresponding author.
E-mail addresses: liuxbing@cgnpc.com.cn (X. Liu), xuefei@cgnpc.com.cn (F. Xue).

https://doi.org/10.1016/j.net.2019.09.001

lattices [6]), these fluences correspond to the peak damage levels of 7 and 15 displacement/atom (dpa). According to the results of SRIM 2012, the irradiation damage depth is 1 μm and the peak damage level is 700 nm. After irradiation, partial specimens irradiated at RT were annealed at 550 °C for 1h in vacuum environment, where the degree of vacuum is lower than 5×10^{-4} Pa.

GIXRD was carried out at Beijing Synchrotron Radiation Facility. The wavelength of X-rays was 0.154 nm. The X-ray scanning range varied from 35 to 55° with a resolution of 0.05°. The of incident angle calculated by penetration depth is 4°. Magnetic hysteresis loops were measured with the vibrating sample magnetometer (VSM) 7407 produced by Lake Shore. The maximum magnetic field intensity is 3000 Oe in the measurement. The disk-shaped specimens with a diameter of 3 mm and a thickness of less than 30 μm was used to reduce the effect of unirradiated part and eliminate the demagnetizing effects brought by the shape and size of specimens.

3. Results and analysis

Fig. 1 shows the GIXRD patterns of unirradiated specimen, irradiated specimens to 7 and 15 dpa at different temperature (RT and 300 °C) and PIA specimens respectively. Due to the perfect solution treatment, the GIXRD pattern of unirradiated specimen shows two face-centered-cubic austenite diffraction peaks of γ(111) and γ(200). No other diffraction peaks were observed. However, a new diffraction peak appears after irradiation. According to the previous studies [4,7,8], this new diffraction peak is corresponding to BCC-phase. With the increasing irradiation damage, a more significant BCC-phase diffraction peak can be observed. Comparing to irradiation at RT, irradiation at 300 °C and PIA will reduce obviously BCC-phase diffraction peak.

Several studies have proved that the formation of BCC-phase will change the magnetic behavior of ASS [9]. Generally, more BCC-phase would bring a stronger magnetization. Therefore, in order to obtain the quantitative information of BCC-phase, the magnetization-magnetic field hysteresis loops with different irradiation damage level under various temperatures are given in Fig. 2. As shown in Fig. 2, the unirradiated specimen remains a small magnetization value with a linear increase in the entire field and no typical hysteresis dependence in ferromagnetic materials was observed. Nevertheless, the irradiated specimens show the hysteresis dependence typical of ferromagnetic materials with a nonlinear variation, which indicates that higher irradiation damage level causes more significant magnetization phenomenon. Under the same damage level, irradiation at RT introduces the largest magnetization, irradiation at 300 °C introduces the next and PIA at 550 °C introduces the least. This tendency is in consistent with the results of GIXRD.

Previously, Takaya et al. [10] indicated that the saturation magnetization (M_s) depends entirely on the volume fraction of the magnetic phase, which suggests that the volume fraction of irradiation-induced BCC-phase can be determined by M_s [11]. In order to evaluate the volume fraction of BCC-phase, the M_s of irradiated specimens was obtained by subtracting the paramagnetic contribution according to the unirradiated specimen. The BCC-phase volume fraction V_{BCC} can be obtained by formula $V_{BCC} = k \cdot (M_{si}-M_{sui})/M$, where k is the correction coefficient, M_{si} and M_{sui} are the M_s of irradiated and unirradiated specimens respectively. The thickness of the VSM specimen L_t is regarded as 25 μm roughly. Considering the approximate distribution of irradiation damage at surface and peak region, irradiation damage is supposed to be uniformly distributed from surface to 1 μm. Therefore, the thickness of irradiation damage layer L_i is about 1 μm. Consequently, we can get the correction coefficient $k = L_t/L_i = 25$. M is the M_s of 100 vol % BCC-phase and take to be about 127emu/g for 316 ASS [12]. Based on this, the obtained BCC-phase volume fraction V_{BCC} is shown in Fig. 3. According to Fig. 3, it can be concluded that the volume fraction of BCC-phase increases with the irradiation damage level. Moreover, high temperature irradiation and PIA can mitigate the formation of BCC-phase. These results suggest that the driving force of irradiation-induced BCC-phase tends to smaller with the increasing irradiation temperature or PIA temperature.

Many studies have been carried out to investigate the BCC-phase formation in ASS under irradiation, but its main driving forces during ion irradiation are not clear. It is known that the BCC-phase

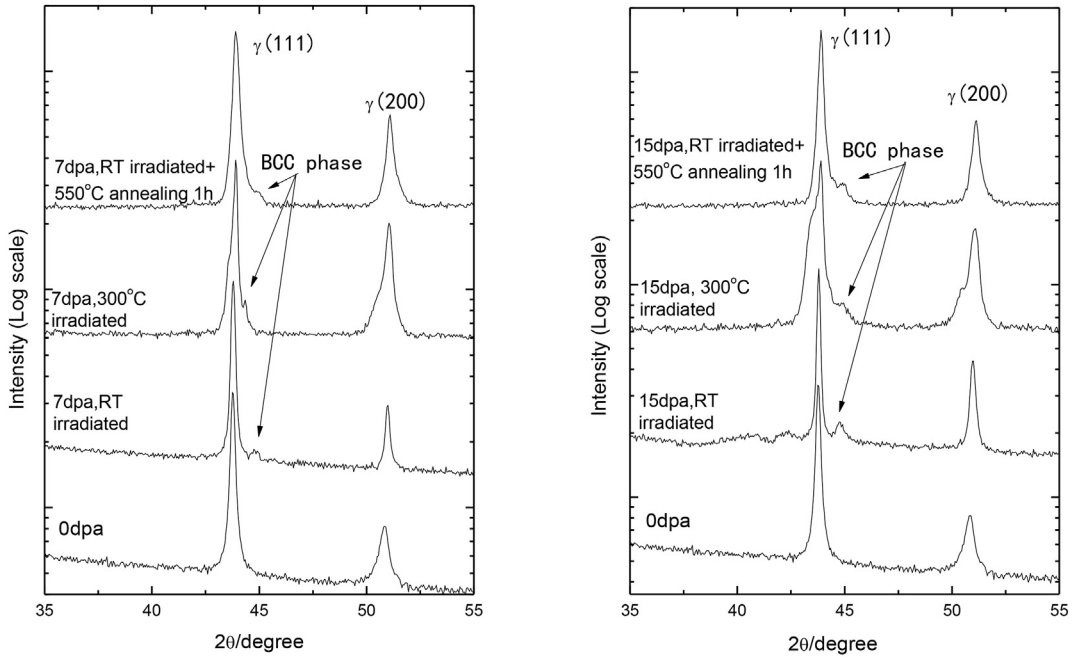

Fig. 1. GIXRD patterns of intensity along Y-axis (Log-scale) under different irradiation condition.

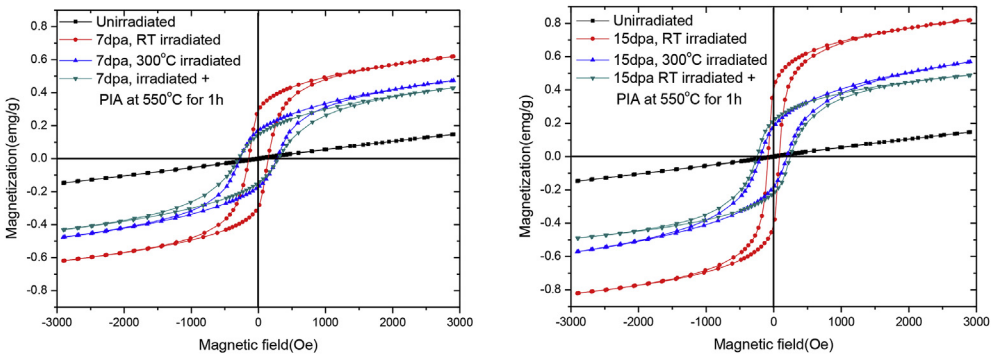

Fig. 2. Variations of hysteresis loops of ASS under different irradiation condition.

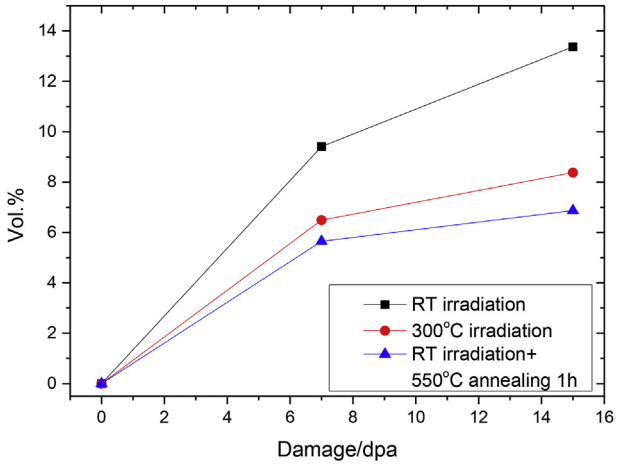

Fig. 3. The BCC-phase volume fraction of ASS with different irradiation temperatures and annealing conditions.

forms in austenitic steels and is usually associated with relief of high internal stress levels and plastic deformation [13]. For ion-irradiated stainless steel, stress relief and plastic deformation come from two different reasons. The first reason is the bubbles formation with Xe irradiation. Our previous studies [14] have observed high density bubbles in ASS after Xe irradiated to 2 dpa at room temperature (as shown in Fig. 4). This high density of bubbles increases the matrix stress and causes the surrounding plastic transformation during the irradiation process. So the BCC-phase formation in Xe irradiated ASS is closely related to the stress relief caused by bubbles. This result is consistent with previous investigation on the phase transformation in inert gas ion irradiation of ASS [15,16]. The second reason is the formation of stacking faults in ion irradiated ASS. The density of stacking faults becomes larger during ion irradiation, which creates an expansion of the lattice and, consequently, an increase of the strains [13]. According to the studies of Fayeulle et al. [17], this stacking faults may cause transformation of the BCC-phase.

Previous studies have observed the BCC-phase formation in thermally sensitized ASS [18–20]. Comparing to the ion irradiation, thermally sensitized ASS does not introduce significant stress relief. This indicates that, besides the contribution of stress relief on BCC-phase formation in ASS, there may be other factors affecting BCC-phase formation in irradiated ASS.

It is known that the phase stability of ASS can be estimated from the Schaeffler diagram, which relates phase stability to the composition [13]. Previously, Johnson et al. [21] indicated that implantations with the ASS constituent elements will shift the positions of the formed alloys to different parts of the Schaeffler diagram. They pointed out that implantations with Fe in ASS will shift the alloy composition towards the martensite corner, favouring the BCC-phase transformations. Implantations with Cr will take the alloy into the two-phase austenite/martensite field, and implantations with nickel will shift the alloy way up into the austenite field away from the martensitic transformations. Nasu and Fujita [22] proposed that the BCC-phase formation in ASS might be induced by preferential sputtering of Ni and Cr which lead to a subsequent reduction in austenite stability of the irradiated surface. In addition, the observation of the reverse BCC-phase to austenite transformation after implantation of nickel or nitrogen in an ASS where BCC-phase was introduced by cold work shows that compositional changes can influence the transformation in accordance with the austenite stabilizing nature of nickel and nitrogen [23]. Moreover, Hayashi and Takahashi [24] suggested that the irradiation-induced depletion of nickel may cause the austenite to

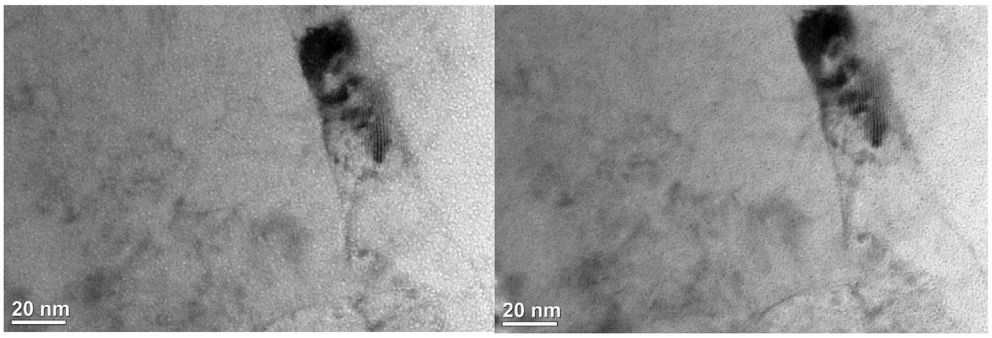

Fig. 4. TEM morphologies of Xe bubbles in irradiated ASS [14]. (left: underfocus, right: overfocus).

BCC-phase transformation. Morisawa et al. [1] and Zhang et al. [25] further point out that the radiation induced segregation (RIS) in austenite phase results in a partial phase transformation from austenite phase to BCC-phase. So based on above understanding, we believe that compositional changes in localized area are another factors affecting the BCC-phase formation. These compositional changes in localized area can be derived from external element implanting or RIS.

In consequence, we concluded that the driving forces for BCC-phase formation during ion irradiation come from two aspects, namely (1) the stress relief caused by gas bubble and defects formation during irradiation; (2) compositional changes in localized area of ASS matrix. So with the increase the irradiation damage, higher stress will be introduced and compositional changes derived from RIS will become significant in austenite matrix, all of which will cause more BCC-phase formation.

For the specimens PIA at 550 °C, according to the discussion above on BCC-phase formation driving force, high annealing temperature will cause the Xe atoms migrating fast and agglomerating easily to large bubbles. As the studies of Sakamoto et al. [7], the equilibrium pressure of Xe inclusion $p = 2\gamma/r$, where γ and r are surface energy of ASS and radius of Xe inclusion, respectively. This indicates that an increase in the diameter of Xe inclusion leads to a decrease of the pressure. Meanwhile, the density of irradiation defects reduced at high temperature, which will decrease the stress in lattice further. So a significant reduction of BCC-phase formation in specimens PIA at 550 °C can be observed.

Previous studies have indicated that the chemical element segregation at grain boundary of ASS will increase with the increasing temperature [26]. This means the effect of chemical driving force on BCC-phase formation will become significant gradually, which seems to be inconsistent with the present results. As the studies of Zhang et al. [27], the effect of stress relief on BCC-phase formation in ASS decreases with the increasing temperature. This suggests that the contribution of stress relief plays a major role in the BCC-phase formation, while the compositional changes have a limited effect. Therefore, the comprehensive results of these two driving forces of BCC-phase formation show a reduction trend. We can deduce that the BCC-phase will not be avoided under high temperature irradiation condition duo to the irreversibility of compositional changes. This result is in accordance with the observation of Chu et al. [13], who indicated that the BCC-phase still exists in ASS irradiated at 873K. Deeper studies are needed to give a further understanding.

4. Conclusion

The ASS specimens were irradiated with 6 MeV Xe ions to two doses of 7 and 15 dpa at room temperature and 300 °C. Then partial irradiated specimens were annealed at 550 °C. The formation of BCC-phase in ASS after irradiation is identified by GIXRD analysis. The quantitative information of BCC-phase is given by VSM data. It is indicated that higher irradiation damage level will cause more BCC-phase. Irradiation at high temperature and PIA can suppress the BCC-phase formation. The driving forces of the BCC-phase formation during ion irradiation come from two aspects, namely (1) the stress relief caused by gas bubble and stacking faults formation; (2) compositional changes in ASS matrix.

Acknowledgements

This research is supported by the National Key Research and Development Program of China (grant No. 2016YFB0700401), the National Natural Science Foundation of China (grant No. 11675123 and 11775255) and Natural Science Foundation of Jiangsu Province of China (grant No. BK20171222).

The authors would like to thank the 320 kV High-voltage Platform in Institute of Modern Physics for ion irradiation experiments and Beijing Synchrotron Radiation Facility 1W1A Diffusion Scattering Station in Institute of High Energy Physics for the help on GIXRD.

References

[1] J. Morisawa, M. Otaka, M. Kodama, et al., J. Nucl. Mater. 302 (2002) 66–71.
[2] Shigeru Takaya, Yuji Nagae, Tsunemitsu Yoshitake, et al., E-J. Adv. Mainten. 1 (2009) 44–51.
[3] B.Z. Margolin, I.P. Kursevich, A.A. Sorokin, et al., Strength Mater. 42 (2010) 144–153.
[4] Hiroshi Kinoshita, Heishichiro Takahashi, Dwi Gustiono, et al., Mater. Trans. 48 (2007) 924–930.
[5] J.P. Biersack, L.G. Haggmark, Nucl. Instrum. Methods 174 (1980) 257–269.
[6] ASTM 521-96, Standard Practice for Neutron Radiation Damage Simulation by Charged-Particle Irradiation, 2003.
[7] I. Sakamoto, N. Hayashi, B. Furubayashi, H. Tanoue, J. Appl. Phys. 68 (9) (1990) 4508–4512.
[8] I. Sakamoto, N. Hayashi, H. Tanoue, Surf. Coat. Technol. 65 (1994) 133–136.
[9] M.N. Gussev, J.T. Busby, L. Tan, F.A. Garner, J. Nucl. Mater. 448 (2014) 294–300.
[10] Shigeru Takaya, Ichiro Yamagata, Shoichi Ichikawa, et al., Int. J. Appl. Electromagn. Mech. 33 (2010) 1335–1342.
[11] Lefu Zhang, Seiki Takahashib, Yasuhiro Kamada, Scr. Mater. 57 (2007) 711–714.
[12] E. Menendez, J. Sort, M.O. Liedke, et al., J. Mater. Res. 24 (2009) 565–573.
[13] Fengmin Chu, Minghui Song, Kazutaka Mitsuishi, et al., Jpn. Soc. Electron Microsc. 51 (2002) 231–234.
[14] Chaoliang Xu, Xiangbing Liu, Fei Xue, et al., Fusion Eng. Des. 133 (2018) 125–129.
[15] W. Van Renterghem, A. Al Mazouzi, S. Van Dyck, J. Nucl. Mater. 413 (2011) 95–102.
[16] M. Chai, W. Lai, Z. Li, W. Feng, Acta Metall. Sin.(Engl. Lett.). 25 (2012) 29–39.
[17] S. Fayeulle, D. Treheux, Appl. Surf. Sci. 25 (1986) 288–304.
[18] E.P. Butler, M.G. Burke, Acta Metall. 34 (3) (1986) 557–570.
[19] Alexandre La Fontaine, Hung-Wei Yen, Patrick Trimby, et al., Corros. Sci. 85 (2014) 1–6.
[20] Y. Kamada, T. Mikami, S. Takahashi, et al., J. Magn. Magn. Mater. 310 (2007) 2856–2858.
[21] E. Johnson, A. Johansen, L. Sarholt-kristensen, et al., Nucl. Instrum. Methods Phys. Res. B 19/20 (1987) 171–176.
[22] S. Nasu, F.E. Fujita, Hyperfine Interact. 29 (1986) 1279–1282.
[23] Rong-shan Wanga, Chao-liang Xu, Xiang-bing Liu, et al., J. Nucl. Mater. 457 (2015) 130–134.
[24] N. Hayashi, T. Takahashi, Appl. Phys. Lett. 41 (1982) 1100–1101.
[25] Lefu Zhanga, Yasuhiro Kamadaa, Hiroaki Kikuchi, et al., J. Magn. Magn. Mater. 271 (2004) 402–408.
[26] Hyung-Ha Jin, Eunsol Ko, Sangyeob Lim, et al., J. Nucl. Mater. 493 (2017) 239–245.
[27] Lefu Zhang, Seiki Takahashi, Yasuhiro Kam102ada, et al., J. Mater. Sci. 40 (2005) 2709–2711.